



HAL
open science

Thermal fatigue and collapse of waxy suspensions

Diogo E V Andrade, Philippe Coussot

► **To cite this version:**

Diogo E V Andrade, Philippe Coussot. Thermal fatigue and collapse of waxy suspensions. *Rheologica Acta*, 2020, 59 (5), pp.279-289. 10.1007/s00397-020-01202-y . hal-03249715

HAL Id: hal-03249715

<https://enpc.hal.science/hal-03249715v1>

Submitted on 4 Jun 2021

HAL is a multi-disciplinary open access archive for the deposit and dissemination of scientific research documents, whether they are published or not. The documents may come from teaching and research institutions in France or abroad, or from public or private research centers.

L'archive ouverte pluridisciplinaire **HAL**, est destinée au dépôt et à la diffusion de documents scientifiques de niveau recherche, publiés ou non, émanant des établissements d'enseignement et de recherche français ou étrangers, des laboratoires publics ou privés.

Thermal fatigue and collapse of waxy suspensions

Diogo E. V. Andrade^{1,2} · Philippe Coussot¹

Received: 25 November 2019 / Revised: 14 February 2020 / Accepted: 17 February 2020
© Springer-Verlag GmbH Germany, part of Springer Nature 2020

Abstract

Due to the existence of a continuous (percolating) network of weak interparticle bonds in a liquid, wax suspensions can behave as “soft breakable (brittle) solids”: under the action of either a large stress over a short time or oscillating low stress (fatigue test), the initially solid network of these materials is broken and dispersed in the liquid, which turns them into abruptly (“collapse”) and irreversibly to a low viscous fluid. Here we show that the rheological behavior of these materials is not only impacted by the temperature but also by the history of the temperature. The elastic modulus and the yield stress increase when the temperature is decreased, and the data for different concentrations (ranging from 7 to 50 wt% of wax in oil) and temperatures as a function of the distance to the critical temperature associated with the transition to liquid state, fall along a master curve, which shows some equivalence between temperature and concentration. More surprisingly, the elastic modulus in the linear regime and the yield stress are dependent on the minimum temperature the material has experienced during its preparation. As a consequence of these different characteristics, an original rheological behavior so far essentially observed with very different materials (metals) results, namely *thermal fatigue*: when the material is submitted to temperature cycling (small temperature amplitude test), the material progressively weakens during each elementary thermal cycle and can finally “collapse” after a sufficient number of cycles, i.e., the elastic modulus in the linear regime decreases from 10^6 to 10^3 Pa. These findings could have implications in the start-up flow of waxy oils in pipelines since with the help of this technique, the material strength (e.g., the yield stress) and consequently the pressure required to resume the flow can be reduced considerably just by imposing thermal cycles.

Keywords Waxy suspensions · Brittle solids · Thermal cracking · Thermal fatigue

Introduction

The production and transportation of waxy crude oil is a challenge in offshore scenarios. The crude oils, that experience high temperatures in the reservoirs, are submitted to low temperatures during the transportation by pipelines, which are in contact with the seabed at around 4 °C (Smith and Ramsden 1978; Huang et al. 2011). During the flow in the pipelines, the oil loses heat to the environment and at a given temperature—called WAT (wax appearance temperature)—the heaviest

normal hydrocarbon molecules precipitate out in the solution as crystal structures (Paso et al. 2005). At high temperatures, the crude oils behave as Newtonian fluids (Wardhaugh and Boger 1991; Venkatesan et al. 2005), whereas, below the WAT, the solid crystals precipitated in the solution are responsible for three main issues in the production process: (i) the crystals give a non-Newtonian behavior to the material increasing the material viscosity and, as a consequence, the required pumping power to keep the flow also increases (Marchesini et al. 2012); (ii) these solids wax can deposit in the inner surface of the pipelines, in these cases, the PIG (pipeline inspection gauges) must be used to remove the paraffin deposited and the deposition rate must be known in order to determine the wax pigging frequency (Aijejina et al. 2011); (iii) when the flow is interrupted, the crystals can entrap the oil and yield a solid-like structure to the material, in this case, one must know the strength of the solid structure after the stoppage in order to determine the required pressure to break down the structured material and to resume the flow (Visintin et al. 2005a).

✉ Philippe Coussot
philippe.coussot@ifsttar.fr

¹ Laboratoire Navier (ENPC, Univ Gustave Eiffel, CNRS), 77455 Mame-la-Vallée, France

² Research Center for Rheology and Non-Newtonian Fluids—CERNN, Postgraduate Program in Mechanical and Materials Engineering—PPGEM, Federal University of Technology-Paraná—UTFPR, R. Deputado Heitor Alencar Furtado, 5000 Bloco N-Ecoville, Curitiba, PR 81280-340, Brazil

The knowledge of the rheological behavior of waxy oil is fundamental to design the pumps and the pipelines and to improve the production and transportation process. Although extensive research has been conducted over the past five decades, there are many points regarding the rheological behavior that are not clear in the literature. The majority of the authors agree that these materials present a yield stress at low temperatures, in the sense that after resting for some time, it is necessary a stress larger than a minimum stress to restart the flow. Some authors say that waxy oils are thixotropic materials (Visintin et al. 2005b; de Souza Mendes and Thompson 2012; Teng and Zhang 2013; Dimitriou and McKinley 2014) while others state that waxy oils must be understood as irreversible time-dependent materials since after the shear, the material does not completely recover the viscosity when the applied shear rate is decreased and does not recover the initial solid-like structure at rest (Rønningsen 1992, 2012; Mendes et al. 2015; Andrade and Coussot 2019).

It is well known that waxy oils are thermal and shear-history dependent (Wardhaugh and Boger 1987). In other words, the different temperatures, cooling rates, and shear applied in the material during the cooling interfere in the crystallization process (nucleation and crystals growth), affecting the morphology of the crystals (Rønningsen et al. 1991; Paso et al. 2005; Yi and Zhang 2011; Andrade et al. 2018) and, as a consequence, influence the macroscopic behavior of the waxy oil at the end of the cooling. The thermal and shear histories are usually evaluated by varying the initial (Smith and Ramsden 1978; Marchesini et al. 2012; Jemmett et al. 2013; Andrade et al. 2015; Dalla et al. 2019) and the final (Davenport and Somper 1971; Hou and Zhang 2010; Mendes et al. 2017) temperature of the cooling, the cooling rate (Lee et al. 2008; Mendes et al. 2017; Andrade et al. 2018), the applied shear during cooling (Venkatesan et al. 2005; Lin et al. 2011; Mendes et al. 2017), and the resting time at the final temperature (Wardhaugh and Boger 1991; Chang et al. 2000; Silva and Coutinho 2004; Mendes et al. 2017). As a general conclusion, it seems that decreasing the final temperature, or increasing the concentration of wax, the material yield stress increases because under these conditions more crystals are formed; the resting time may play a role depending on the composition of the oil, in other words, it seems that for the majority of the crude oils, increasing the resting time at the final temperature increases the strength of the structure (Lin et al. 2011; Van Der Geest et al. 2019); on the other hand, for model waxy oils, the material strength varies in the first minutes of rest and then the elastic modulus and the material yield stress become independent on the resting time (Andrade and Coussot 2019); regarding the dynamic cooling, the final structure of the material is much affected by the shear during the cooling, i.e., the material strength (elastic modulus and yield stress) after dynamic cooling is order of magnitudes lower than the strength of the material obtained after static

cooling (Lin et al. 2011; Andrade et al. 2015). Finally, it is interesting to note a non-monotonic variation of the strength of waxy oils in the solid regime as a function of the initial cooling temperature (Marchesini et al. 2012; Andrade et al. 2015; Dalla et al. 2019), the cooling rate (Lee et al. 2008; Andrade et al. 2018), and the shear stress applied during the cooling (Venkatesan et al. 2005).

Here we intend to clarify the impact of thermal changes on waxy crude by focusing on a model system. These materials are commonly used as model materials to study the rheological behavior of waxy crude oil (Singh et al. 2001; Dimitriou et al. 2011; Zhao et al. 2012; Mendes et al. 2015; Andrade et al. 2017) that are transported in subsea pipelines, lubricating mineral oil (Webber 1999, 2001) which can reach low temperatures in some applications, and in a recent study (Andrade and Coussot 2019), it was also proposed that model waxy oils might be used as a model system to simulate and explain natural catastrophic events such as landslides and avalanches.

Although we cannot claim that this material behaves exactly as a typical waxy crude, it can be expected that some fundamental qualitative aspects of the behavior of the model wax suspensions will be found also with waxy crude oils, since both material types are basically made of waxy matter in suspension in a liquid and which crystallize progressively as the temperature is decreased. Moreover, the use of these simple model systems might make it possible to distinguish more easily the original trends of these systems without being too much blurred by various complications due to some additional components.

Model waxy oils are systems composed of paraffin wax mixed in mineral oil. As mentioned previously, these materials behave as a Newtonian fluid at high temperatures, when all the paraffins are dissolved in the oil, and below the WAT, the paraffins precipitate in the oil as wax crystals giving a non-Newtonian behavior to the material. In a previous study (Andrade and Coussot 2019), it was shown that, when cooled at rest (without external stress perturbation in the sample during the cooling), such a material type may be seen as a brittle solid presenting very high elastic modulus (up to 10^6 Pa) and very low critical strain (in the order of $5 \cdot 10^{-5}$) around which the material leaves the linear regime, and finally the material transforms into a simple liquid after some significant shear (Andrade and Coussot 2019). The impact of concentration at a given temperature was analyzed, suggesting that during cooling, the crystals formed are connected by interparticle solid bonds that structure the sample and give the solid-like behavior to the material. Here we intend to analyze how the thermal history impacts these properties.

We first recall in more detail the main characteristics of the material used. Then we further analyze the influence of the temperature in the solid regime of the waxy model oil: we demonstrate that the elastic modulus variations when the temperature decreases at a given concentration are similar to its

163 variations when the concentration is increased at a given tem- 209
164 perature. It is then shown that the waxy oil presents a thermal 210
165 memory in the sense that the elastic modulus in the linear 211
166 regime and the yield stress are dependent on the minimum 212
167 temperature the material has experienced. Finally, a thermal 213
168 fatigue test (small temperature amplitude tests) may be used to 214
169 strongly alter the material, as for metals (Starling and Branco 215
170 1997; Persson et al. 2005) and bitumen (Soenen and 216
171 Vanelstraete 2003; Kumar-Das et al. 2012), but here this leads 217
172 to the liquefaction of the material. We start with the experi- 218
173 mental section, followed by the results, discussion, and then 219
174 the main conclusions. 220

175 Experimental section

176 The model wax oils analyzed are composed of a paraffin wax 225
177 (Sigma Aldrich 327212 CAS-No:8002-74-2, with a melting 226
178 point between 58 and 62 °C) mixed in a mineral oil (Sigma 227
179 Aldrich 330779 CAS-No: 8042-47-5) as proposed in previous 228
180 studies (Dimitriou et al. 2011; Mendes et al. 2015; Andrade 229
181 et al. 2018; Andrade and Coussot 2019). The samples were 230
182 stored in an oven at 60 °C, a temperature higher than the solid- 231
183 liquid equilibrium temperature for these materials. It is worth 232
184 remembering that when mixed in the mineral oil, the wax 233
185 solubilizes in the liquid and the thermodynamic solid-liquid 234
186 equilibrium temperature, $T_{eq,SL}$, turns a function of the con- 235
187 centration of wax in oil. For example, the $T_{eq,SL}$ is 32.0, 36.0, 236
188 42.6, for, respectively, 5, 10, and 20 wt% of wax in oil 237
189 (Andrade et al. 2017). All the rheometrical tests were per- 238
190 formed in the stress-controlled rotational Malvern Kinexus 239
191 Pro+ rheometer, equipped with serrated (0.5 mm groove 240
192 depth) parallel plates (50 mm diameter and 1 mm gap), in 241
193 which the temperature was controlled by a Peltier- 242
194 thermostatic bath system. Prior to all experiments, the sample 243
195 was loaded with the aid of a syringe on the rheometer; at this 244
196 time, the parallel plates and the syringe were also at 60 °C in 245
197 order to prevent precipitation of crystals during loading. 246

198 As different protocols were used, we are going to describe 247
199 the experiments before showing each result. But it is important 248
200 to emphasize that in all the experiments, the rate of change of 249
201 temperature (cooling or heating rate) was kept at 1.0 °C/min 250
202 and that all the cooling and heating processes were performed 251
203 statically, i.e., with no shear imposed to the material. 252

204 Results

205 Material structure in the initial state

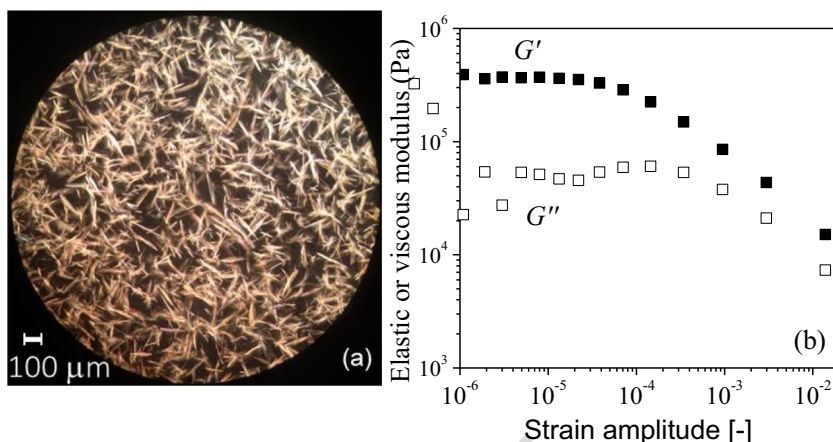
206 Let us first recall the main characteristics of the waxy oil 253
207 suspensions in the solid regime, under fixed thermal history. 254
208 During the cooling, the material reaches the WAT (wax 255

appearance temperature) and the paraffins start to precipitate 209
as crystals structures in the material. It is known that the higher 210
the concentration of wax in oil, the higher the WAT is 211
(Andrade et al. 2017) and as the temperature decreases, more 212
solid paraffins crystallize in the oil. If the cooling is performed 213
quiescently, at a certain point, the crystals can percolate and 214
form a structure in the material. From microscopy image ob- 215
tained at 25 °C for 8 wt% after imposing a cooling rate of 216
1 °C/min from 60 °C (Fig. 1), the crystals appear to present 217
a needle-like morphology which likely forms a network of 218
inter-particle bonds that is responsible for the initial solid- 219
like behavior of the material. During a stress amplitude oscil- 220
latory sweep, the material presents a very high elastic modulus 221
(G') in the linear regime, in the order of $4 \cdot 10^5$ Pa (see Fig. 1), 222
when compared to the typical values for soft-jammed systems 223
(say, a few hundred Pascals, see Coussot et al. (2006)). The 224
material then leaves the linear region (i.e., G' starts to decrease 225
with the stress imposed to the sample) at a very low strain 226
amplitude, in the order of $5 \cdot 10^{-5}$, and the elastic modulus 227
drops by several orders of magnitude. These trends suggested 228
to consider that we are dealing with brittle soft solids. 229

230 Still under the same thermal history, it was shown that the 231
elastic modulus in the linear regime starts to increase rapidly 232
beyond a critical concentration of wax up to about 10 wt%. In 233
this range, increasing the concentration just increases the num- 234
ber of needles but does not affect the needle size (see Andrade 235
and Coussot (2019)). The variation of the elastic modulus as a 236
function of the concentration increment above the critical one 237
appeared to be consistent with a percolation phenomenon in a 238
sol-gel transition (De Gennes 1980). Around 10 wt%, the 239
elastic modulus seems to reach a plateau (in the order of 240
 $2 \cdot 10^6$ Pa) while the size of the needles rapidly increases, but 241
the structure observed for concentrations beyond 10 wt% is 242
similar to that observed at smaller concentrations with just a 243
scale change of the elements. Besides the fact that the elastic 244
modulus reaches a plateau, the material yield stress goes on 245
increasing beyond the concentration of 10 wt%. The data pre- 246
sented in Andrade and Coussot (2019) concerning the elastic 247
modulus and the yield stress are summarized in Fig. 2. 248

249 Under a given thermal history, the solid to fluid transi- 250
tion for such a material appears to be very abrupt. After 251
preparation, a constant stress is imposed for some time and 252
we follow the resulting deformation in time. At the end of 253
this test, the material is heated again then cooled down, and 254
a new stress value is applied. The material appears to re- 255
main in a solid state for sufficiently small stresses, i.e., the 256
deformation remains limited (see Fig. 3). Beyond a critical 257
stress, the material behavior is completely different: the 258
deformation initially slowly increases, then increases sud- 259
denly and dramatically, giving the aspect of a vertical jump 260
in a strain vs time diagram: the strain increases up to sev- 261
eral orders of magnitude typically in less than one second 262
(see Fig. 3). Thus, when the material reaches a critical 263

Fig. 1 Microscopic aspect of the sample (a) and dynamic moduli as a function of the strain amplitude in an oscillatory sweep stress amplitude performed at 1 Hz (b). Image and test performed at 25 °C after the static cooling from 60 to 25 °C, with a cooling rate of 1 °C/min and a resting time of 10 min. In the image, the bright needles are the wax crystals and the black region is the oil. 8 wt% of paraffin in oil



262 strain ($\gamma_c \approx 0.1$), the material breaks and presents a “col-
 263 lapse” in the sense that the shear strain evolves orders of
 264 magnitude in a very short time. It is interesting to note that
 265 a similar behavior was already reported by Wardhaugh and
 266 Boger (1991) using crude oils. Then the material reaches a
 267 liquid state, with a behavior close to a Newtonian one with
 268 a viscosity equal to a few times that of the suspending oil
 269 (Andrade and Coussot 2019). Note that this solid-liquid
 270 transition appears to be irreversible over a time of obser-
 271 vation of several days, since this liquid behavior is ob-
 272 served to persist during such a period. In other words, it
 273 seems that after the breakdown of the interparticle bonds,
 274 the structure is not recoverable unless the sample is heated
 275 to dissolve all the paraffins in the oil and cooled again to
 276 the initial solid state. It is also worth noting that a similar
 277 collapse may be obtained through a fatigue test, i.e., stress
 278 oscillations of amplitude smaller than the yield stress
 279 (Andrade and Coussot 2019). Note that a similar trend
 280 (irreversible breakage and the fatigue process acting in
 281 the material) was observed recently for soft solid (i.e., pro-
 282 tein gels) (Saint-Michel et al. 2017).

Influence of temperature on the waxy oil rheological behavior

283
 284
 285 Let us now analyze the influence of temperature on the solid
 286 behavior of waxy oils for different wax concentrations. All the
 287 samples were cooled with a constant cooling rate of 1 °C/min
 288 from 60 °C to the temperature of interest with no perturbation
 289 in the sample and then the dynamic moduli were measured.
 290 Due to the brittleness of the material, the dynamic moduli
 291 were determined by imposing a stress amplitude sweep with
 292 a trigger in the rheometer that stops the measurement when the
 293 strain amplitude reaches 1.10^{-5} in order to avoid some break-
 294 down of the bonds in this measurement. After the oscillatory
 295 test, the sample is cooled again to the next temperature with
 296 the same cooling rate (1 °C/min) and rested again during
 297 10 min before the measurement of the dynamic moduli. This
 298 procedure was repeated for all the samples in the range of
 299 temperature presented in Fig. 4. It is important to emphasize
 300 that in all these measurements, the material is in thermody-
 301 namic equilibrium, in other words, if we rest the material for
 302 longer time at some given temperature, the dynamic modulus

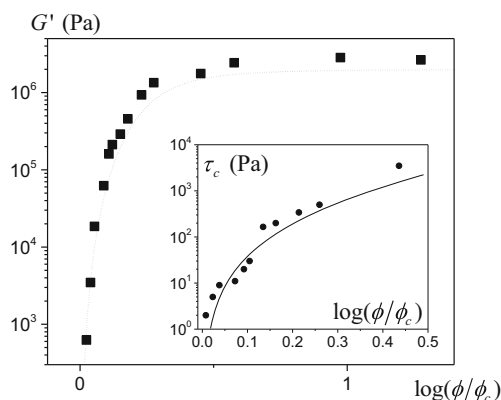


Fig. 2 Elastic modulus (main figure) and yield stress (inset) as a function of the mass concentration of wax in oil ϕ . ϕ_c is the critical concentration (here equal to 5.5%) below which the value of the elastic modulus appeared negligible. Data from Andrade and Coussot (2019)

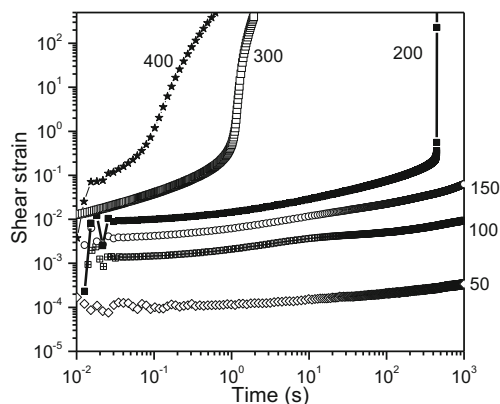


Fig. 3 Creep test performed after the same thermal history that was imposed in the experiments performed in Fig. 1 ($T_i = 60$ °C, cooling rate 1 °C/min and $T_f = 25$ °C). For each test, the material is heated and cooled again in order to get the same initial state before each experiment. 8 wt% of paraffin in oil. Data from Andrade and Coussot (2019)

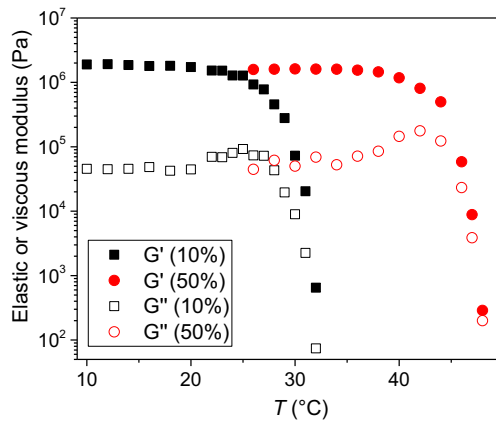


Fig. 4 G' and G'' as a function of temperature for 10 and 50 wt% of wax in oil

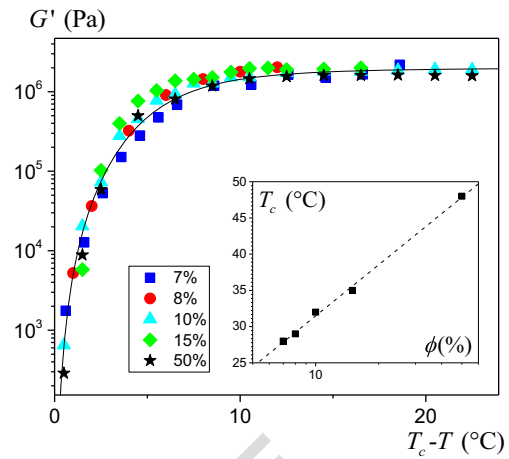


Fig. 5 Elastic modulus for different concentrations as a function of the temperature, and critical temperature (T_c) as a function of concentration (inset). The continuous line is Eq. (2). The dashed line in the inset is Eq. (1)

303 remains constant (see Fig. 11 in the Appendix). This means
 304 that waxy suspensions do not present the aging process as
 305 noticed for many yield stress materials (Joshi and Petekidis
 306 2018) in the sense that if the waxy model oil is cooled to a
 307 fixed temperature, the elastic modulus evolves up to a fixed
 308 value just after the cooling and then does not evolve anymore.

309 For a given concentration, the elastic modulus starts to
 310 increase below some critical temperature T_c , then it rapidly
 311 tends to a plateau at a high level, i.e. G'_0 (see Fig. 4).
 312 Remarkably, the shape of $G'(T)$ for another (for example
 313 smaller) concentration is very similar but simply shifted
 314 towards lower temperatures (see Fig. 4). It is also worth
 315 emphasizing that the plateau value for the elastic modulus
 316 does not depend on the concentration. This means that
 317 there is a maximum elastic modulus in the linear regime
 318 that cannot be overcome whatever the concentration. This
 319 value appears to be close to that for the pure wax (see
 320 Andrade and Coussot (2019)). Under these conditions,
 321 we can rescale all the data for the different concentrations
 322 along a master curve representing $G'(T_c - T)$ (see Fig. 5).
 323 Figure 5 just shows the results of G' obtained using the
 324 same protocol as the used in the experiments of Fig. 4,
 325 but now for five different concentrations of waxy in oil
 326 and changing the axis to $T_c - T$. This allows to determine
 327 the value of T_c [°C], which increases with the concentra-
 328 tion, ϕ [%], (see inset of Fig. 5), and whose variations may
 329 be well represented by the following empirical equation:

$$T_c = 8 + 23.4 \times \log \phi \quad (1)$$

330

332 On the other hand, remarking that $G' - G'_0$ varies as a power-
 333 law when $T_c - T$ tends to zero, with an exponent around 3, we
 334 suggest to represent the rescaled data for the elastic modulus
 335 in the following way (see Fig. 5):

$$1/G' = \left[1/G'_0 + 0.0002 \times (T_c - T)^{-3} \right] \quad (2)$$

338

339

340 On the other side, the yield stress for the different tem-
 341 peratures may be determined from a series of creep tests
 342 under various stress values, such as those done in Fig. 3,
 343 for a material which has been cooled at the desired value.
 344 However, this procedure is extremely long, since each yield
 345 stress determination requires to impose a large set of stress
 346 values, each time preparing again the material in the same
 347 state according to the fixed thermal history. In order to
 348 obtain more directly a good estimation of the yield stress,
 349 we imposed a slowly increasing stress ramp and retained as
 350 the yield stress the stress value for which the shear strain
 351 exhibits an abrupt increase. This method consisting to im-
 352 pose a slow flow is more direct on some aspects as it pro-
 353 vides directly a “yield stress value”, whereas the creep tests
 354 only provides a range in which lies the yield stress. On the
 355 other side, we can fear that considering the particular brittle
 356 behavior of these pastes, the result may be somewhat af-
 357 fected by the procedure, but the critical stress obtained from
 358 a series of creep tests and from such a slow stress ramp are
 359 rather close (see Fig. 12 in the Appendix).

359 The influence of the temperature on the yield stress for
 360 three different concentrations is presented in Fig. 6 in which
 361 each experimental point corresponds to a sample that was
 362 heated to the initial cooling temperature in order to dissolve
 363 all the paraffin in oil and cooled again to the desired temper-
 364 ature. The yield stress also starts to increase from zero below
 365 some critical concentration (see inset of Fig. 6), obviously
 366 similar to the critical one observed for the elastic modulus.
 367 However, here we can observe that the yield stress does not
 368 reach a plateau at some temperature; it goes on increasing as
 369 the temperature decreases. As a consequence, the data for the
 370 yield stress are not simply shifted towards lower temperatures;
 371 when the concentration decreases, the yield stress additionally
 372 increases (see inset of Fig. 6). It happens that the yield stress

369Q2

372

373 rescaled by the concentration simply falls along a master curve
 374 as a function of the difference between the current and the
 375 critical temperatures (see Fig. 6). The data can then well be
 376 represented by the following equation (see Fig. 6):

$$\tau_c = 100\phi(T_c - T)^2 \quad (3)$$

378 The consistency of this representation of the data can be
 379 checked by comparing their prediction of the variation of the
 380 elastic modulus and yield stress as a function of the concentra-
 381 tion with the data obtained previously (see Fig. 2). Let us
 382 now assume that the temperature T_0 is fixed. In the expres-
 383 sions (2) and (3) the parameter is now T_c , which varies as a
 384 function of ϕ according to (1). In addition, we can define a
 385 critical concentration ϕ_c below which the material is not in a
 386 solid state at the temperature T_0 : $\phi_c = 10^{(T_c - 8)/23.4}$. T_0 : $\phi_c =$
 387 $\exp(T_0 - 9)/10.1$. From this equation and the expression (1)
 388 we deduce

$$T_c - T_0 = 23.4 \times \log \phi / \phi_c \quad (4)$$

390 which may be inserted in (2) and (3) to obtain the expressions
 392 of the elastic modulus and yield stress as a function of the
 393 concentration. These expressions appear to rather well corre-
 394 spond to the data obtained at a fixed temperature in a previous
 395 study (see Fig. 2). It is important to emphasize that these
 396 empirical equations are valid for the model waxy system in-
 397 vestigated in this manuscript.

398 Thermal memory

399 It is well known in literature that waxy oils are thermal history
 400 dependent in the sense that the final cooling temperature and
 401 the cooling rate affect the rheological behavior of the material
 402 (see "Introduction"). As far as we know, the effect of a partial

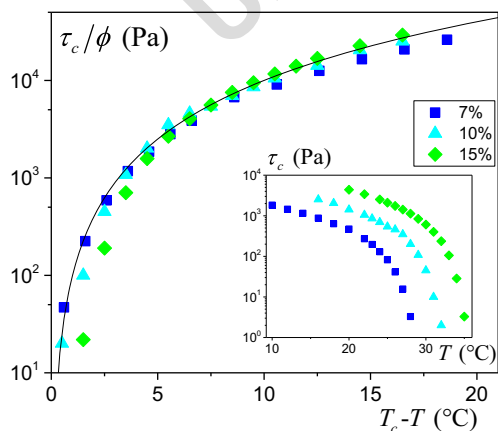


Fig. 6 Impact of temperature on yield stress. The inset shows the yield stress as a function of temperature for different concentrations. The main figure presents the same data with the yield stress rescaled by the concentration and the temperature difference with regard to the critical temperature. The continuous line is Eq. (3)

403 temperature cycle, i.e., temperature decrease then increase,
 404 has not been studied. Let us consider a material prepared
 405 through a given thermal history (i.e., cooling from 60 to
 406 25 °C and resting for 10 min), and to which we impose a stress
 407 level, with now in addition a temperature increase with a con-
 408 stant heating rate of 1 °C/min. Looking at the strain vs tem-
 409 perature evolution, we see that as in the case of constant tem-
 410 perature for a stress beyond the yield stress (Fig. 3), the ma-
 411 terial starts to flow abruptly at some critical temperature value
 412 during the temperature increase as presented in Fig. 7. The
 413 higher the shear stress applied, the lower is the temperature
 414 for which this breakdown appears. The main point is that
 415 surprisingly, the minimum temperature experienced by the
 416 sample (in this case 25 °C) affects the yield stress of the ma-
 417 terial: the magnitude of the stress required to break up the
 418 structure and to start-up the flow decreases considerably when
 419 the minimum temperature attained is decreased. For example,
 420 the material breaks at 100 Pa when heated from 25 °C to
 421 around 28 °C while the yield stress of this material when
 422 cooled from high temperature to 28 °C is 201 Pa. In order to
 423 facilitate the analysis, the inset table in Fig. 7 compares the
 424 yield stress measured after the cooling from high temperature
 425 to the desired temperature (values of the Fig. 6 for 10 wt%
 426 measured at isothermal condition) and the values obtained in
 427 Fig. 7 in which the sample experienced the minimum tempera-
 428 ture of 25 °C (measured at non-isothermal condition, i.e.,
 429 during the heating). We can clearly see that the critical stress
 430 is much affected by the minimum temperature.

431 These results suggest an impact of the minimum tempera-
 432 ture reached during the thermal history. In order to more di-
 433 rectly observe this effect, we now follow the evolution of G'
 434 during the cooling down to a given temperature and the

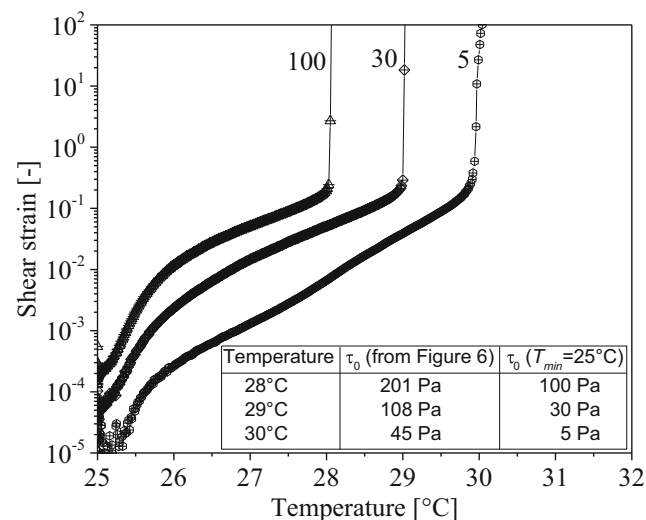


Fig. 7 Analysis of the behavior of the waxy oil during the heating. After cooling, a given stress (indicated in Pascals along the curves in the graph) is applied while the sample is heated at a constant heating rate of 1 °C/min. The values obtained from Fig. 6 were determined at isothermal conditions. $\phi = 10$ wt%

435 subsequent heating of the material under our usual heating rate
 436 of 1 °C/min (Fig. 8a). Note that during this process, the elastic
 437 modulus was measured after 10 min of rest at each tempera-
 438 ture of analysis, so that we can expect to have reached a ther-
 439 mal equilibrium at each step of the process. Surprisingly, de-
 440 spite this, the material strength is not only a function of the
 441 temperature but also of the thermal history that it has experi-
 442 enced. The G' decreases below its initial values associated
 443 with the temperature decrease (see Fig. 8a). Moreover, the
 444 lower the minimum temperature experienced by the sample,
 445 the greater is the lowering of G' during the temperature in-
 446 crease (see Fig. 8a). It nevertheless seems that decreasing the
 447 minimum temperature to lower than 15 °C does not affect
 448 much more the structure of the material. A similar behavior
 449 was observed for other concentrations (see Fig. 13 in the
 450 Appendix) and also when the experiment was performed with
 451 a serrated surface Couette geometry (results not presented). It
 452 is important to emphasize that without this thermal change,
 453 i.e., if the sample is kept at the same temperature (e.g., 25 °C)
 454 and we apply similar oscillation history, we get a constant
 455 value of G' (see Fig. 11 in the Appendix) and not a decrease
 456 in the elastic modulus as presented in Fig. 8.

457 A similar effect is observed for the yield stress (Fig. 8b).
 458 In this case, in these experiments we used the same proce-
 459 dure presented in Fig. 6 but now with a thermal history in
 460 which the sample was cooled until a minimum temperature and
 461 heated until the temperature of test. It is important to empha-
 462 size that for each point, after breakdown, the sample is
 463 heated again to 60 °C in order to dissolve all the wax in
 464 oil and the new thermal history was imposed to the materi-
 465 al. In other words, the data presented in Fig. 8b were not
 466 obtained successively for the same sample. We can see that
 467 for the two minimum temperatures analyzed (25 and
 468 20 °C), the thermal history has a great effect on the materi-
 469 al yield stress. For example, the yield stress observed at
 470 28 °C through our standard direct cooling procedure is
 471 201 Pa, but drops to 12 Pa, if the material has been cooled
 472 to 20 °C then heated back to 28 °C.

Collapse of the structure by imposing thermal cycle

473

474 Since the material presents a thermal memory, it seems likely
 475 that we can weak the structure by oscillating the temperature.
 476 In order to check that, after the standard cooling (60 to 25 °C),
 477 we impose thermal cycles which consist to lower the temper-
 478 ature following a linear ramp, then keeping a constant value,
 479 and increasing again the temperature along a short linear ramp
 480 to go back to the initial value, then again a plateau, a decrease,
 481 and so on (see Fig. 9). It is important to mention that all the
 482 thermal history is imposed without any stress perturbation in
 483 the sample, and that the dynamic moduli are measured over a
 484 relatively short time at the end of each cycle (at a temperature
 485 of 25 °C) by imposing a stress amplitude sweep with a trigger
 486 in the rheometer that stops the measurement when the strain
 487 amplitude reaches 10^{-5} . After each experiment, we could see
 488 that even after the thermal cycles, the material is still in the
 489 linear regime to strain smaller than 10^{-5} .

490 We can see that the dynamic moduli measured at 25 °C
 491 decreases after imposing each cycle in the sample (Fig. 10).
 492 This decrease is faster at the beginning then a continuous
 493 decrease of G' is observed down to values (e.g., after the
 494 20th cycle) which are three orders of magnitude lower than
 495 the initial one, and of the order of those observed after the
 496 material collapse, i.e., around $2 \cdot 10^3$ Pa (as presented in
 497 Andrade and Coussot (2019)). In other words, we can “col-
 498 lapse” the structure (decreasing the G' from 10^6 to 10^3 Pa)
 499 without imposing any stress in the sample, just by thermal
 500 cycles. Moreover, the smaller the minimum temperature used
 501 in these cycles the stronger the decrease of G' along the suc-
 502 cessive cycles (see Fig. 10), so that the collapse is reached
 503 sooner. It is important to emphasize that different protocols
 504 were tested (not shown in order to facilitate the understanding
 505 of the main message of the paper), and the thermal cycle also
 506 affects the mechanical properties of the material at the mini-
 507 mum temperature of the cycle. But in this case, the lower the
 508 minimum temperature, the greater is the number of cycles
 509 required to weaken the structure of the material.

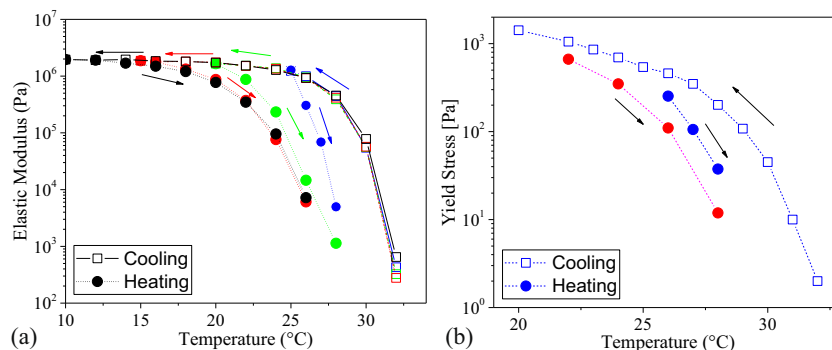


Fig. 8 a Elastic modulus as a function of temperature during the cooling and the heating phases for different minimum temperatures (from right to left) $T_{\min} = 25$ °C (blue), 20 °C (green), 15 °C (red), and 10 °C (black)). b

Yield stress (see procedures of determination in the text) as a function temperature for two different minimum temperatures ($T_{\min} = 25$ °C (blue) and 20 °C (red)). $\phi = 10$ wt%

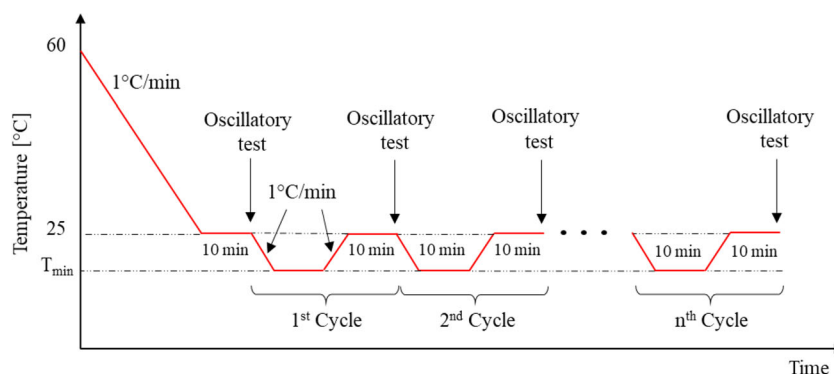


Fig. 9 Scheme of the thermal histories used to analyze the influence of the thermal cycle on the waxy oil. The material was cooled from 60 to 25 °C, then a thermal cycle was imposed between 25 °C and T_{min}

(minimum temperature). In all the temperature ramps, the rate of change of temperature is 1 °C/min regardless of whether cooling or heating is applied

510 **Discussion**

511 With our waxy oils we can see a kind of “low temperature
 512 cracking” in which the material strength is affected by the
 513 minimum temperature experienced by the sample (see Figs.
 514 7 and 8) and also a thermal fatigue process, in which oscillat-
 515 ing the temperature the material weakens and suffers a “col-
 516 lapse” without any external stress imposed in the material
 517 (Fig. 10). The thermal fatigue cracking is a well-known pro-
 518 cess in metals (Starling and Branco 1997; Persson et al. 2005)
 519 in which the materials fail when exposed to hot work thermal
 520 cycles. In these cases, the authors state that the materials are
 521 subjected to thermal gradients during the fast temperature
 522 changing and, as a consequence, the thermal expansions and
 523 contractions are not homogenous throughout the sample, gener-
 524 ating different deformation and residual stress in the materi-
 525 al. As a consequence, these thermal cycles can lead to fatigue
 526 cracking at the surface of the material. It is an important issue
 527 for die casting and warm forging industries. On the other
 528 hand, the low-temperature cracking and the thermal fatigue
 529 cracking at low temperatures have been studied in bitumen
 530 to understand failure in asphalt pavements (Soenen and
 531 Vanelstraete 2003; Kumar-Das et al. 2012). In these cases,
 532 during the cooling, the bitumen is able to shrink and relax
 533 the stress up to a certain temperature, but upon further cooling,
 534 the bitumen stiffens and is no longer able to relax the stress
 535 through a viscous mechanism. These low temperatures gener-
 536 ate thermal cracking in the material that is also generated by
 537 several thermal cycles.

538 In order to discuss the physical origin of this thermal fati-
 539 gue for our waxy oils, we have to refer to their specific
 540 structure in the solid regime (as compared to metals): this is
 541 a rather “open” structure built on a percolated network of
 542 needles linked by solid bonds. Moreover, the macroscopic
 543 behavior relies on the links between the needles, as only the
 544 links are broken during the solid-liquid transition, i.e., the
 545 needles remain intact (see Andrade and Coussot (2019)).

This implies that what occurs inside the needles as a result 546
 of temperature variations should play a negligible role; they 547
 can be considered as rigid, and formed during the first thermal 548
 cycle after preparation. Under these conditions, the impact of 549
 temperature on the elastic modulus and yield stress is associ- 550
 ated with the exact state of crystallization of the material com- 551
 posing the links between needles. If the structure could simply 552
 be considered as formed of the association of a number of 553
 crystals increasing when the temperature decreases, decreas- 554
 ing values of the yield stress, and the elastic modulus would be 555
 obtained for increasing temperatures. This is indeed what we 556
 observe. If in addition each crystal formation or fusion is ob- 557
 tained at the same given temperature, for low temperature 558
 variations, the thermal history cannot have any impact: the 559
 current temperature solely imposes the structure state, hence 560
 the mechanical strength of the material. If the temperature of 561
 crystallization is lower than the temperature of fusion, there 562
 might be some hysteresis, but this will only play a role during 563
 the first thermal cycle, with little to no long-term evolution. 564

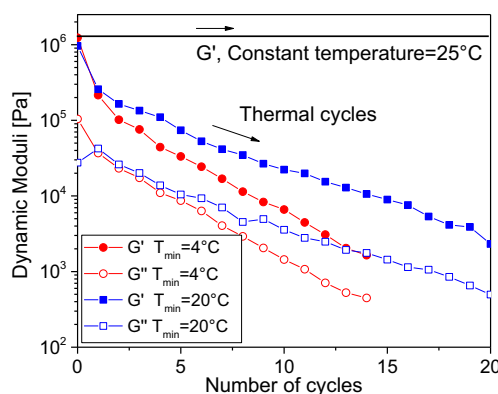


Fig. 10 Dynamic moduli measured at 25 °C after thermal cycles (see procedure in Fig. 9). The first point (Number of cycles = 0) corresponds to the end of the cooling at rest from 60 to 25 °C and the other points correspond to the subsequent measurements after an increasing number of cycles. The upper continuous line represents the value of G' at a constant temperature, i.e., without thermal cycle. $\phi = 10$ wt%

565 This implies that, in order to explain the thermal
 566 fatigue of these materials, we necessarily have to con-
 567 sider that some steps of the process alter the material
 568 more than strictly in relation with crystallization and
 569 fusion of some elements of the structure of the material
 570 composing the links between the needles. In a way sim-
 571 ilar to the thermal fatigue in metals, we can suggest that
 572 the partial fusion of some crystals during the step of
 573 temperature increase, alters the structure of the material
 574 at other locations than the strict crystal under consider-
 575 ation. This could be due to a slighter density increase
 576 obtained after crystallization, tending to compact the
 577 structure, while the fusion of some crystals under a
 578 slight temperature increase would lead to a slight den-
 579 sity decrease tending to break some “contacts” (or more
 580 globally speaking, propagate fracture) between crystals
 581 otherwise not altered by the thermal cycle. The succes-
 582 sion of such cycles would then break more and more
 583 such contacts.

584 **Conclusions**

585 The main conclusions of the work can be summarized as
 586 follows:

- 587 • The waxy oil is a brittle material whose mechanical prop-
 588 erties are affected by the minimum temperature experi-
 589 enced by the material; for example, the elastic modulus
 590 analyzed at 28 °C can decrease three orders of magnitude
 591 and the yield stress can decrease two orders of magnitude
 592 just by cooling statically the material to 20 °C and heating
 593 again to 28 °C.
- 594 • Lower minimum temperatures imply a more pronounced
 595 impact of the thermal cycle;
- 596 • If the material is thermally cycled, we can observe
 597 thermal fatigue in the material. In other words, with-
 598 out imposing any stress in the material, just by suc-
 599 cessive thermal cycles, the structure “collapses” and
 600 the material liquefies.
- 601 • This behavior could lead to important implications in the
 602 start-up flow of waxy oils, since we show that it is possible
 603 to decrease considerably the material yield stress just by
 604 cycling the temperature of the material.

605 Understanding the exact physical origin of this behavior
 606 would require to develop imaging technique at a very low
 607 scale inside the wax link between needles.

608 **Acknowledgments** D.E.V.A acknowledges CAPES (Coordination for
 609 the Improvement of Higher Education Personnel - Brazil) (Process:
 610 88881.170234/2018-01) for the Postdoctoral Fellowship.

Appendix

Dynamic moduli as a function of time

613 After the static cooling from 60 to 25 °C with 1 °C/min of
 614 cooling rate, the material was kept at rest during 10 min and then
 615 a constant stress amplitude oscillatory test was applied in the
 616 material in the linear regime (stress amplitude = 10 Pa and fre-
 617 quency = 1 Hz) and the dynamic moduli were analyzed over time
 618 (Fig. 11). It is possible to see that in the linear regime—and if the
 619 temperature is not changed—the strength of the material (e.g., the
 620 elastic modulus) remains constant over time.

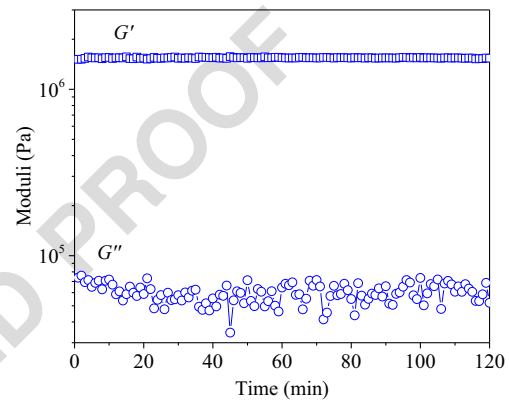


Fig. 11 G' and G'' as a function of time measured at a constant temperature of 25 °C after a static cooling with $T_i = 60$ °C and cooling rate of 1 °C/min. $\phi = 10$ wt%

Yield stress: creep test × stress ramp

622 As discussed in the text, the yield stress may be determined
 623 from a series of creep tests under various stress values, as
 624 presented for 8 wt% (Fig. 3). However, with this procedure,
 625 a precise value of the yield stress can be obtained only after a
 626 great number of tests. As in this work, we are analyzing the
 627 influence of the concentration and different thermal histories
 628 on the yield stress; determining the yield stress with a series of
 629 creep tests would be a very slow process and almost prohibi-
 630 tive due to the time need to get the yield stress for each con-
 631 dition. In order to obtain more directly a good estimation of
 632 the yield stress, we imposed a slowly increasing stress ramp
 633 and retained as the yield stress, the stress value for which the
 634 shear strain exhibits an abrupt increase. Just to compare, we
 635 are showing again the results of creep test (Fig. 12a) presented
 636 previously (Andrade and Coussot 2019) for 10 wt% of wax in
 637 oil. In these tests, we can see that the material breaks if a stress
 638 of 500 Pa or higher is applied in the sample. If the same
 639 thermal history is applied in the sample but instead of a plateau
 640 of stress, we impose a stress ramp, one can see at which stress
 641 the material breaks analyzing the shear strain as a function of
 642 stress (Fig. 12b). We can see that for the stress ramp, the
 643 material was broken when the stress reached around 550 Pa.

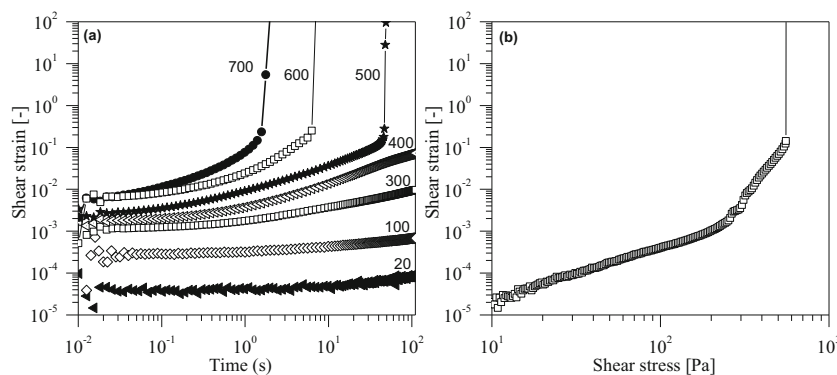


Fig. 12 Experiments performed with 10 wt% of wax in oil, $T_i = 60\text{ }^\circ\text{C}$, $1\text{ }^\circ\text{C/min}$ of cooling rate, $T_f = 25\text{ }^\circ\text{C}$, and 10 min of resting time. **a** Shear strain as a function of time in the creep test. Before each plateau of stress, the sample is heated and cooled again using the same thermal history.

(Results presented in data presented in Andrade and Coussot (2019)). **b** Shear strain as a function of shear stress in the stress ramp stress. In this measurement, the stress was increased logarithmically at a rate of one order of magnitude per each 10 min

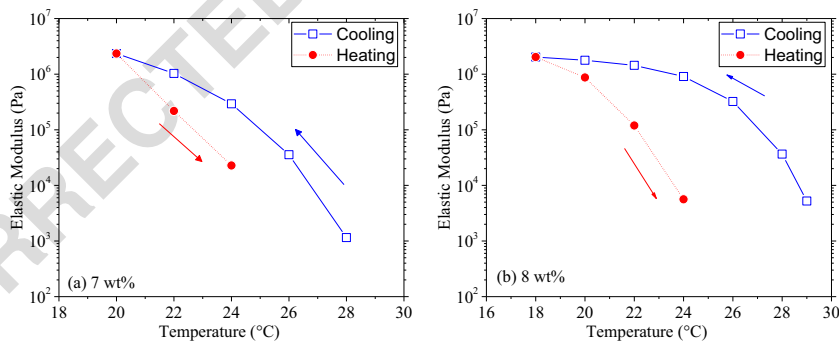
644 **Thermal memory for different concentrations**

645 The same experiment presented for 10 wt% (see Fig. 8a) was
646 performed for two other concentrations, 7 wt% (see Fig. 13a)

and 8 wt% (see Fig. 13b). We can see that the minimum
647 temperature also affects the strength of the material for other
648 concentrations.

650
651

Fig. 13 G' as a function of temperature during the cooling (squares in blue) and for the same sample during the heating (stars in red) for **a** $\phi = 7\text{ wt}\%$ and **b** $\phi = 8\text{ wt}\%$



652 **References**

653 Aiyejina A, Chakrabarti DP, Pilgrim A, Sastry MKS (2011) Wax formation
654 in oil pipelines: a critical review. *Int J Multiphase Flow* 37:671–
655 694. <https://doi.org/10.1016/j.ijmultiphaseflow.2011.02.007>
656 Andrade DEV, Coussot P (2019) Brittle solid collapse to simple liquid for
657 a waxy suspension. *Soft Matter* 15:8766–8777. <https://doi.org/10.1039/c9sm01517e>
658 Andrade DEV, da Cruz ACB, Franco AT, Negrão COR (2015) Influence
659 of the initial cooling temperature on the gelation and yield stress of
660 waxy crude oils. *Rheol Acta* 54:149–157. <https://doi.org/10.1007/s00397-014-0812-0>
661 Andrade DEV, Marcelino Neto MA, Negrão COR (2018) Non-
662 monotonic response of waxy oil gel strength to cooling rate. *Rheol*
663 *Acta* 57:673–680. <https://doi.org/10.1007/s00397-018-1108-6>
664 Andrade DEV, Marcelino Neto MA, Negrão COR (2017) The importance
665 of supersaturation on determining the solid-liquid equilibrium tem-
666 perature of waxy oils. *Fuel* 206:516–523. <https://doi.org/10.1016/j.fuel.2017.06.042>

Chang C, Boger DV, Nguyen QD (2000) Influence of thermal history on
670 the waxy structure of statically cooled waxy crude oil. *SPE J* 5:2–3.
671 <https://doi.org/10.2118/57959-PA>
672 Coussot P, Tabuteau H, Chateau X et al (2006) Aging and solid or liquid
673 behavior in pastes. *J Rheol (N Y N Y)* 50:975–994. <https://doi.org/10.1122/1.2337259>
674 Dalla LFR, Soares EJ, Siqueira RN (2019) Start-up of waxy crude oils in
675 pipelines. *J Nonnewton Fluid Mech* 263:61–68. <https://doi.org/10.1016/j.jnnfm.2018.11.008>
676 Davenport TC, Somper RSH (1971) The yield value and breakdown of
677 crude oil gels. *J Inst Pet* 57:86–105
678 De Gennes P (1980) Percolation : quelques systemes nouveaux. *J Phys*
679 *Colloq* 41:17–26
680 de Souza Mendes PR, Thompson RL (2012) A critical overview of
681 elasto-viscoplastic thixotropic modeling. *J Nonnewton Fluid Mech*
682 187–188:8–15. <https://doi.org/10.1016/j.jnnfm.2012.08.006>
683 Dimitriou CJ, McKinley GH (2014) A comprehensive constitutive law
684 for waxy crude oil: a thixotropic yield stress fluid. *Soft Matter* 10:
685 6619–6644. <https://doi.org/10.1039/c4sm00578c>
686
687
688

- 689 Dimitriou CJ, McKinley GH, Venkatesan R (2011) Rheo-PIV analysis of
690 the yielding and flow of model waxy crude oils. *Energy Fuel* 25:
691 3040–3052. <https://doi.org/10.1021/ef2002348>
- 692 Hou L, Zhang J (2010) A study on creep behavior of gelled Daqing crude
693 oil. *Pet Sci Technol* 28:690–699. [https://doi.org/10.1080/](https://doi.org/10.1080/10916460902804648)
694 [10916460902804648](https://doi.org/10.1080/10916460902804648)
- 695 Huang Z, Lu Y, Hoffmann R et al (2011) The effect of operating temper-
696 atures on wax deposition. *Energy Fuel* 25:5180–5188. [https://doi.](https://doi.org/10.1021/ef201048w)
697 [org/10.1021/ef201048w](https://doi.org/10.1021/ef201048w)
- 698 Jemmett MR, Magda JJ, Deo MD (2013) Heterogeneous organic gels:
699 rheology and restart. *Energy Fuel* 27:1762–1771. [https://doi.org/10.](https://doi.org/10.1021/ef3014629)
700 [1021/ef3014629](https://doi.org/10.1021/ef3014629)
- 701 Joshi YM, Petekidis G (2018) Yield stress fluids and ageing. *Rheol Acta*
702 57:521–549. <https://doi.org/10.1007/s00397-018-1096-6>
- 703 Kumar-Das P, Jelagin D, Birgisson B, Kringos N (2012) Micro-
704 mechanical investigation of low temperature fatigue cracking behav-
705 iour of bitumen. In: 7th RILEM international conference on crack-
706 ing in pavements. pp 1281–1290
- 707 Lee HS, Singh P, Thomason WH, Fogler HS (2008) Waxy oil gel break-
708 ing mechanisms: adhesive versus cohesive failure. *Energy Fuel* 22:
709 480–487. <https://doi.org/10.1021/ef700212v>
- 710 Lin M, Li C, Yang F, Ma Y (2011) Isothermal structure development of
711 Qinghai waxy crude oil after static and dynamic cooling. *J Pet Sci*
712 *Eng* 77:351–358. <https://doi.org/10.1016/j.petrol.2011.04.010>
- 713 Marchesini FH, Aliche AA, de Souza Mendes PR, Ziglio CM (2012)
714 Rheological characterization of waxy crude oils: sample prepara-
715 tion. *Energy Fuel* 26:2566–2577. <https://doi.org/10.1021/ef201335c>
- 716 Mendes R, Vinay G, Coussot P (2017) Yield stress and minimum pres-
717 sure for simulating the flow restart of a waxy crude oil pipeline.
718 *Energy Fuel* 31:395–407. [https://doi.org/10.1021/acs.energyfuels.](https://doi.org/10.1021/acs.energyfuels.6b02576)
719 [6b02576](https://doi.org/10.1021/acs.energyfuels.6b02576)
- 720 Mendes R, Vinay G, Ovarlez G, Coussot P (2015) Reversible and irre-
721 versible destructuring flow in waxy oils: an MRI study. *J Non-*
722 *Newtonian Fluid Mech* 220:77–86. [https://doi.org/10.1016/j.](https://doi.org/10.1016/j.jnnfm.2014.09.011)
723 [jnnfm.2014.09.011](https://doi.org/10.1016/j.jnnfm.2014.09.011)
- 724 Paso K, Senra M, Yi Y et al (2005) Paraffin polydispersity facilitates
725 mechanical gelation. *Ind Eng Chem Res* 44:7242–7254. [https://](https://doi.org/10.1021/ie050325u)
726 doi.org/10.1021/ie050325u
- 727 Persson A, Hogmark S, Bergström J (2005) Thermal fatigue cracking of
728 surface engineered hot work tool steels. *Surf Coat Technol* 191:216–
729 227. <https://doi.org/10.1016/j.surfcoat.2004.04.053>
- 730 Rønningsen HP (1992) Rheological behaviour of gelled, waxy North Sea
731 crude oils. *J Pet Sci Eng* 7:177–213. [https://doi.org/10.1016/0920-](https://doi.org/10.1016/0920-4105(92)90019-W)
732 [4105\(92\)90019-W](https://doi.org/10.1016/0920-4105(92)90019-W)
- 733 Rønningsen HP (2012) Rheology of petroleum fluids. *Annu Trans Nord*
734 *Rheol Soc* 20:11–18
- 735 Rønningsen HP, Bjørndal B, Hansen AB, Pedersen WB (1991) Wax
736 precipitation from North Sea crude oils. 1. Crystallization and dis-
737 solution temperatures, and Newtonian and non-Newtonian flow
738 properties. *Energy Fuel* 5:895–908. [https://doi.org/10.1021/](https://doi.org/10.1021/ef00030a019)
739 [ef00030a019](https://doi.org/10.1021/ef00030a019)
- 740 Saint-Michel B, Gibaud T, Manneville S (2017) Predicting and assessing
741 rupture in protein gels under oscillatory shear. *Soft Matter* 13:2643–
742 2653. <https://doi.org/10.1039/C7SM00064B>
- 743 796
- Silva JAL, Coutinho JAP (2004) Dynamic rheological analysis of the
744 gelation behaviour of waxy crude oils. *Rheol Acta* 43:433–441.
745 <https://doi.org/10.1007/s00397-004-0367-6>
- Singh P, Venkatesan R, Fogler HS, Nagarajan NR (2001) Morphological
746 evolution of thick wax deposits during aging. *AIChE J* 47:6–18.
747 <https://doi.org/10.1002/aic.690470103>
- 748 748
- Smith PB, Ramsden RMJ (1978) The prediction of oil gelation in sub-
749 marine pipelines and the pressure required for restarting flow. In:
750 *Europeans Offshore Petroleum Conference & Exhibition*
- 751 Soenen H, Vanelstraete A (2003) Performance indicators for low temper-
752 ature cracking. In: *Sixth International RILEM Symposium on*
753 *Performance Testing and Evaluation of Bituminous Materials*. pp
754 458–464
- 755 Starling CMD, Branco JRT (1997) Thermal fatigue of hot work tool steel
756 with hard coatings. *Thin Solid Films* 308–309:436–442. [https://doi.](https://doi.org/10.1016/S0040-6090(97)00600-7)
757 [org/10.1016/S0040-6090\(97\)00600-7](https://doi.org/10.1016/S0040-6090(97)00600-7)
- 758 Teng H, Zhang J (2013) A new thixotropic model for waxy crude. *Rheol*
759 *Acta* 52:903–911. <https://doi.org/10.1007/s00397-013-0729-z>
- 760 Van Der Geest C, Guersoni VCB, Bannwart AC (2019) Experimental
761 study of the time to restart the flow of a gelled waxy crude in
762 rheometer and pipeline. *J Pet Sci Eng* 181:106247. [https://doi.org/](https://doi.org/10.1016/j.petrol.2019.106247)
763 [10.1016/j.petrol.2019.106247](https://doi.org/10.1016/j.petrol.2019.106247)
- 764 Venkatesan R, Nagarajan NR, Paso K et al (2005) The strength of paraffin
765 gels formed under static and flow conditions. *Chem Eng Sci* 60:
766 3587–3598. <https://doi.org/10.1016/j.ces.2005.02.045>
- 767 Visintin RFG, Lapasin R, Vignati E et al (2005a) Rheological behavior
768 and structural interpretation of waxy crude oil gels. *Langmuir* 21:
769 6240–6249. <https://doi.org/10.1021/la050705k>
- 770 Visintin RFG, Lapasin R, Vignati E, D'Antona P, Lockhart TP (2005b)
771 Rheological behavior and structural interpretation of waxy crude oil
772 gels. *Langmuir* 21:6240–6249. <https://doi.org/10.1021/la050705k>
- 773 Wardhaugh LT, Boger DV (1987) Measurement of the unique flow prop-
774 erties of waxy crude oils. *Chem Eng Res Des* 65:74–83
- 775 Wardhaugh LT, Boger DV (1991) The measurement and description of
776 the yielding behavior of waxy crude oil. *J Rheol* 35:1121–1156.
777 <https://doi.org/10.1122/1.550168>
- 778 Webber RM (1999) Low temperature rheology of lubricating mineral
779 oils: effects of cooling rate and wax crystallization on flow prop-
780 erties of base oils. *J Rheol* 43:911–931. [https://doi.org/10.1122/1.](https://doi.org/10.1122/1.551045)
781 [551045](https://doi.org/10.1122/1.551045)
- 782 Webber RM (2001) Yield properties of wax crystal structures formed in
783 lubricant mineral oils. *Ind Eng Chem Res* 40:195–203. [https://doi.](https://doi.org/10.1021/ie000417d)
784 [org/10.1021/ie000417d](https://doi.org/10.1021/ie000417d)
- 785 Yi S, Zhang J (2011) Relationship between waxy crude oil composition
786 and change in the morphology and structure of wax crystals induced
787 by pour-point-depressant beneficiation. *Energy Fuel* 25:1686–1696.
788 <https://doi.org/10.1021/ef200059p>
- 789 Zhao Y, Kumar L, Paso K, Ali H, Safieva J, Sjöblom J (2012) Gelation
790 and breakage behavior of model wax – oil systems: rheological
791 properties and model development. *Ind Eng Chem Res* 51:8123–
792 8133
- 793 793
- Publisher's note** Springer Nature remains neutral with regard to jurisdic-
794 tional claims in published maps and institutional affiliations. 795